

Operational Monitoring of Radar Differential Reflectivity Using the Sun

IWAN HOLLEMAN

Royal Netherlands Meteorological Institute (KNMI), De Bilt, Netherlands

ASKO HUUSKONEN

Finnish Meteorological Institute, Helsinki, Finland

RASHPAL GILL

Danish Meteorological Institute, Copenhagen, Denmark

PIERRE TABARY

Météo-France, Toulouse, France

(Manuscript received 20 August 2009, in final form 17 December 2009)

ABSTRACT

A method for the daily monitoring of the differential reflectivity bias for polarimetric weather radars is presented. Sun signals detected in polar volume data produced during operational scanning of the radar are used. This method is an extension of that for monitoring the weather radar antenna pointing at low elevations and the radar receiving chain using the sun. This “online” method is ideally suited for routine application in networks of operational radars.

The online sun monitoring can be used to check the agreement between horizontal and vertical polarization lobes of the radar antenna, which is a prerequisite for high-quality polarimetric measurements. By performing both online sun monitoring and rain calibration at vertical incidence, the differential receiver bias and differential transmitter bias can be disentangled. Results from the polarimetric radars in Trappes (France) and Bornholm (Denmark), demonstrating the importance of regular monitoring of the differential reflectivity bias, are discussed.

It is recommended that the online sun-monitoring method, preferably in combination with rain calibration, is routinely performed on all polarimetric weather radars because accurate calibration is a prerequisite for most polarimetric algorithms.

1. Introduction

The issue of differential reflectivity Z_{dr} calibration is crucial for successful applications of a dual-polarization radar (Ryzhkov et al. 2005). For example, Gourley et al. (2006) have found, using an algorithm based on reflectivity and Z_{dr} , that a precision of 0.2 dB in the differential reflectivity still results in 15% errors in the estimated rain rates. Offline sun measurements, where operational scanning is stopped and the radar antenna is pointing at the sun, are generally employed to calibrate the polarimetric

receiving chain (Pratte and Ferraro 1989; Melnikov et al. 2003; Ryzhkov et al. 2005; Zrnić et al. 2006). Pratte and Ferraro (1989) describe an automated procedure for calibration (on receiving) of the radar gain and Z_{dr} using sun pointing. More recently, Melnikov et al. (2003) report the use of dedicated sun scans for monitoring the calibration of Z_{dr} on the polarimetric Weather Surveillance Radar-1988 Doppler (WSR-88D). The required corrections for differences in the noise power and bandwidths between the horizontal and vertical channels are discussed. Results of the solar monitoring during the period of May–December 2002 suggest a Z_{dr} calibration stability better than 0.2 dB (Ryzhkov et al. 2005).

Recently an “online” sun method has been developed, where incidental sun signals are automatically detected in polar volume data generated during operational scanning

Corresponding author address: Iwan Holleman, Royal Netherlands Meteorological Institute, P.O. Box 201, NL-3730 AE De Bilt, Netherlands.
E-mail: i.holleman@science.ru.nl

for monitoring the antenna pointing (Huuskonen and Holleman 2007) and the radar receiving chain (Holleman et al. 2010). The online method allows for daily monitoring of operational radars and networks thereof. In addition it can be applied to archived volume data. Here, we present an extension of the online sun method to the monitoring of differential reflectivity from polarimetric weather radars. Operational polarimetric radars usually possess so-called polarization diversity, meaning that the transmitted radiation is of a fixed polarization and a dual receiver processes horizontal and vertical polarizations simultaneously (Bringi and Chandrasekar 2001). We will discuss the nature of the solar differential reflectivity signals and present a model to interpret them. The daily differential reflectivity biases are compared to those obtained from rain calibration at zenith (Gorgucci et al. 1999). Results from the operational polarimetric radars in Trappes (France) and Bornholm (Denmark) are presented, which clearly demonstrate the importance of the daily monitoring of the differential reflectivity bias. The summary and conclusions are given at the end of the paper.

2. Polarimetric radar data

Data from two polarimetric weather radars in France and Denmark are used in this study.

a. Weather radar in Trappes

Météo-France operates 10 polarimetric Doppler weather radars. The C-band polarimetric weather radar in Trappes (near Paris, France) operates continuously as part of the French radar network. The radar is equipped with linear polarization capabilities, and it simultaneously transmits horizontally and vertically polarized waves. The two receiving channels, which have nearly identical waveguide runs, operate in parallel and thus enable the simultaneous transmission and reception (STAR mode) of polarized signals. Relevant technical parameters of this radar are listed in Table 1 and more details can be found in Gourley et al. (2006).

Every 15 min the radar scans 11 different elevations between 0.4° and 9.5° elevation. The lowest three elevations (0.4° , 0.8° , and 1.5°) are repeated every 5 min. Finally, a zenith scan (90° elevation) for the rain calibration of differential reflectivity is performed every 15 min. Polar volume data of uncorrected reflectivity, radial velocity, spectral width, differential reflectivity, differential phase shift, and copolar correlation coefficient are stored with a range resolution of 240 m and an azimuthal integration angle of 0.5° . A 3-month archive running from 1 March to 31 May 2008 is available for this study.

TABLE 1. Relevant technical parameters of the French and Danish polarimetric weather radars involved in this study.

Parameter	Trappes	Bornholm
Manufacturer	SELEX	EEC
Radar system	Meteor 510AC	DWSR-2501C
Signal processor	CASTOR-2	EDRP 9
Geographical position	48.775°N, 2.009°E	55.113°N, 14.999°E
Wavelength	5.31 cm	5.33 cm
Polarization	H/V	H/V
Beam diameter	1.1°	0.9°
Peak power	250 kW	269 kW
Pulse duration	2.0 μ s	0.8 μ s
Noise level	-112 dBm	-114 dBm
Radar constant	71.0 dB	69.0 dB

b. Weather radar in Bornholm

The Danish Meteorological Institute (DMI) operates two polarimetric Doppler radars and three Doppler radars for weather monitoring. The C-band polarimetric radar on the island Bornholm in the Baltic Sea has been in operation since September 2007. The digital receiver is mounted at the back of the antenna pedestal and the radars are operated in STAR mode as well. Nine elevations between 0.5° and 15.0° are scanned at every 10 min. The range and azimuth resolutions are 500 m and 1.0° , respectively. The polar volume data with the usual Doppler moments plus the differential reflectivity, the differential phase shift, and the copolar correlation coefficient are stored.

A software package based on Huuskonen and Holleman (2007) has run daily since 2008 to monitor both the antenna pointing accuracy (azimuth and elevation) and the receiving chain of all Danish weather radars. For this study the method was extended to monitor the differential reflectivity using the sun signals detected in the polar volume data from Bornholm.

3. Method

a. Automated detection of sun signatures

The automated detection of sun signatures in polar volume data from scanning weather radars is straightforward and it is described in Huuskonen and Holleman (2007) and Holleman et al. (2010). The sun is a continuous source of radio-frequency radiation, and thus it can be recognized by a consistent reflectivity signal at long ranges (e.g., >100 km). To avoid severe refraction and contamination due to scatter from precipitation, elevations below 1° are discarded. The reflectivity factor signal of a sun signature recorded at Trappes is presented in the upper panel of Fig. 1. The reflectivity factor signal is relatively weak (<10 dBZ), and it increases with range because of range standard corrections in the radar signal

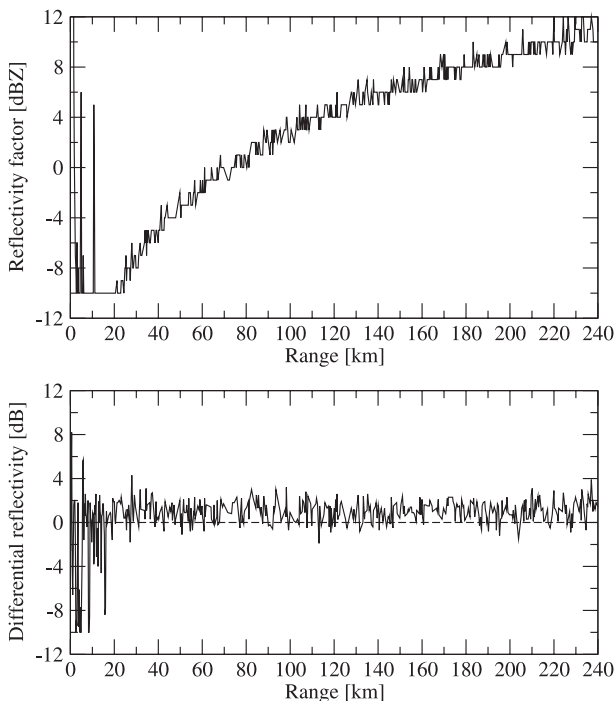


FIG. 1. A-scope plots, i.e., signal vs range, of (top) the reflectivity factor and (bottom) differential reflectivity data for a sun signal as observed by the Trappes radar at 0654 UTC 1 Mar 2008 (el 3.5° and az 104°).

processor. Knowing the applied radar constant and gaseous attenuation correction, the solar power can be calculated from the reflectivity factor data (Huuskonen and Holleman 2007).

The lower panel of Fig. 1 shows the corresponding differential reflectivity data as a function of range. The observed differential reflectivity is constant with range and slightly positive. Because the radio-frequency radiation from the sun is either unpolarized (thermal emission) or circular polarized (sun spots), the differential reflectivity associated with the sun signal should be 0 dB. By simple averaging over range, the differential reflectivity of this individual sun signature is determined to be 1.0 ± 0.9 dB. For all detected sun signals, the range-averaged differential reflectivity and solar power, azimuth and elevation readings, and date-time stamp are stored for further analysis.

b. Analysis of sun signatures

Scatterplots of the sun signals detected by the Trappes radar during March 2008 are presented in Fig. 2. More than 720 sun signatures (about 23 day^{-1}) are depicted in each of these scatterplots. The sun signatures are scattered over roughly 1.5° and 1.2° in azimuth and elevation, respectively. The wider scattering in azimuth is due to the movement of the radar antenna during operational

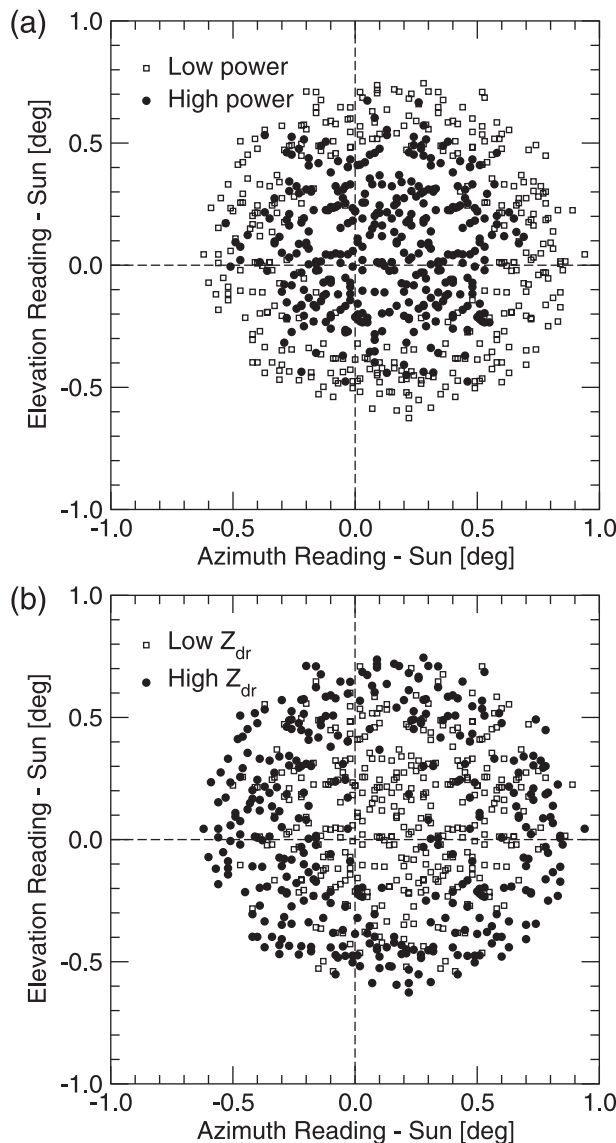


FIG. 2. Scatterplots of the (a) received solar power and (b) differential reflectivity signals collected by the weather radar in Trappes during March 2008. The vertical axis gives the difference between the observed antenna elevation (reading) and the calculated elevation of the sun, and the horizontal axis gives the same for the azimuth. The filled circles and open squares represent the 50% highest and 50% lowest values, respectively.

scanning. The upper scatterplot shows the solar power of the signatures and the filled circles and open squares indicate the 50% highest and 50% lowest values, respectively. The solar power data exhibit a radial pattern with a clear maximum in the center but slightly offset from the origin. This offset points to small biases in the radar antenna alignment. The maximum observed solar power is about 3 dB higher than the lowest values at the edges, and it corresponds to the radar antenna pointing optimally at

the sun. These observations are in accordance with earlier results (Huuskonen and Holleman 2007).

The lower scatterplot of Fig. 2 shows the differential reflectivity using the same convention for the filled and open circles. The differential reflectivity data exhibit a more homogeneous pattern but a minimum is still seen in the center. The minimum differential reflectivity of -0.1 dB is roughly 1.7 dB lower than the highest values. A similar scatterplot is obtained from data of the Bornholm radar (not shown). It has been suggested that differential reflectivity can be biased (up to a few decibels) for weak signals because of noise (Bringi and Chandrasekar 2001). Melnikov et al. (2003) have noted that differences in noise bandwidths of the dual receivers can cause differential reflectivity biases for weak narrowband signals. However, this is different for wideband signals and the differential reflectivity of solar signals $Z_{\text{dr}}^{\text{sun}}$ can be written as

$$Z_{\text{dr}}^{\text{sun}} = 10 \log_{10} \left[\frac{g_h B_h (S_h + N_h)}{g_v B_v (S_v + N_v)} \right], \quad (1)$$

where g and B represent the receiver gain in linear units and bandwidth in hertz, respectively. The spectral sun power is given by S in watts per hertz and the spectral noise power by N . Subscripts h and v denote the respective values for the horizontal and vertical polarization receivers. For the (unpolarized) sun it holds that $S_h \simeq S_v$ (differential attenuation is usually negligible), and for receivers with comparable noise temperatures (e.g., within 25%) it holds that $N_h \simeq N_v$ (within 1 dB). Under these assumptions Eq. (1) reduces to

$$Z_{\text{dr}}^{\text{sun}} = \Delta R_{hv} + 10 \log_{10} \frac{B_h}{B_v}, \quad (2)$$

where the differential receiver bias is defined as $\Delta R_{hv} \equiv 10 \log_{10}(g_h/g_v)$. Thus, for dual receivers with equal bandwidths (B_h and B_v) the differential reflectivity bias of the sun signals is due to differences in receiver gain between the two polarization channels. Note that we are actually determining the bias of the linear depolarization ratio (Bringi and Chandrasekar 2001), which only depends on the receiving chain.

The model given in Eq. (2) is able to explain a constant bias, but it cannot explain the curved pattern visible in the scatterplot of Fig. 2. The pattern is isotropic, just like the pattern of the received solar power, and hence we will seek an explanation by considering the antenna patterns. If the horizontal and vertical polarization lobes of the radar antenna were fully identical, the received differential reflectivity would be constant. Any differences between the antenna's lobes show up as a curved

pattern, as will be detailed in the next section. The observed pattern in Fig. 2 is, therefore, interpreted as a reflection of the (imperfect) spatial overlap between the horizontal and vertical polarization lobes of the antenna (see section 6.2 of Bringi and Chandrasekar 2001).

c. Modeling of sun signatures

All solar signatures detected per day are analyzed using the linear model and fitting procedure described extensively in Huuskonen and Holleman (2007) and Holleman et al. (2010). However, the interpretation of the fit parameters is different. The differential reflectivity (dB) as a function of the radial distance to the antenna beam axis is modeled by

$$Z_{\text{dr}}(x, y) \equiv a_x x^2 + a_y y^2 + b_x x + b_y y + c, \quad (3)$$

where the coordinates in azimuth x and elevation y (matching the axes of Fig. 2) are defined as

$$x = \text{az}_{\text{read}} - \text{az}_{\text{sun}} \quad \text{and} \quad (4)$$

$$y = \text{el}_{\text{read}} - \text{el}_{\text{sun}}, \quad (5)$$

where ‘‘az’’ and ‘‘el’’ refer to the azimuth and elevation, respectively, and ‘‘read’’ indicates the angle reading of the radar antenna. By differencing the equation for the solar power $p_h(x, y)$ received in the horizontal channel [Eq. (16) in Huuskonen and Holleman (2007)] and a similar equation for that in the vertical channel, the above equation for Z_{dr} can be interpreted and the five parameters are then given by

$$\frac{1}{\Delta_{\text{az},v}^2} - \frac{1}{\Delta_{\text{az},h}^2} = \frac{a_x}{40 \log_{10} 2}, \quad (6)$$

$$\frac{1}{\Delta_{\text{el},v}^2} - \frac{1}{\Delta_{\text{el},h}^2} = \frac{a_y}{40 \log_{10} 2}, \quad (7)$$

$$x_0 = -\frac{b_x}{2a_x}, \quad (8)$$

$$y_0 = -\frac{b_y}{2a_y}, \quad \text{and} \quad (9)$$

$$\hat{Z}_{\text{dr}}^{\text{sun}} = c - \frac{b_x^2}{4a_x} - \frac{b_y^2}{4a_y}, \quad (10)$$

where Δ represents the 3-dB antenna beamwidth in degrees and subscripts az and el refer to values in azimuth and elevation planes. Parameter $\hat{Z}_{\text{dr}}^{\text{sun}}$ describes the estimated solar differential reflectivity (in dB) when the radar antenna and the sun are perfectly aligned ($x = x_0$

and $y = y_0$). When the horizontal and vertical polarization lobes of the antenna would perfectly match, curvature parameters a_x and a_y would be zero and a simple average of the differential reflectivity data would be sufficient. In all other cases, the curvature provides information on the difference between the widths of the horizontal and vertical polarization lobes. Equation (3) is linear in the parameters a_x to c , and thus the sun signature data can easily be fitted to this equation by the least squares method. The standard deviation of the estimated differential reflectivity, calculated during the fit from the chi-square residual (Press et al. 1992), serves as a sensitive quality measure of the daily analyses.

d. Rain calibration

The calibration of differential reflectivity using polarimetric properties of rain has first been demonstrated by Gorgucci et al. (1999). Differential reflectivity measurements at vertical incidence are used to calibrate Z_{dr} because this polarimetric quantity is intrinsically zero for raindrops at 90° elevation. If Z_{dr} (dB) measured by this method is not zero, then this value is considered to be the system bias. The differential reflectivity from raindrops observed at zenith is interpreted as the sum of the receiver and transmitter differential biases:

$$Z_{dr}^{\text{rain}} = \Delta R_{hv} + \Delta T_{hv}, \quad (11)$$

where ΔT_{hv} represents the difference between the transmitted power in horizontal and vertical polarizations. For rain calibration the Trappes radar scans the zenith every 15 min. These scans were analyzed to detect rainy episodes using criteria of the reflectivity factor (between 18 and 50 dBZ) and of the copolar correlation coefficient (>0.97). Differential reflectivity data within the 2–6-km range were used, and an average over all azimuths was made to avoid the direction-dependent bias associated with the potential canting of the particles and ground clutter contributions (Gorgucci et al. 1999). Note that when bandwidths of the horizontal and vertical polarization receivers are equal the transmitter differential bias can be determined from the differential reflectivity of the sun and that of the rain calibration.

4. Results and discussion

In this section, results from the operational polarimetric radars in Trappes and Bornholm are presented and discussed.

a. Trappes radar

Prior to the daily analysis of the volume data, the curvature (a_x, a_y) was estimated by simultaneously analyzing

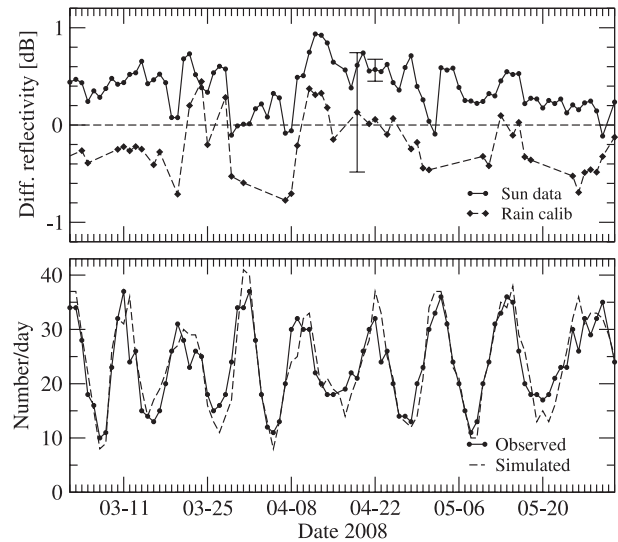


FIG. 3. Daily analysis of the sun signatures observed by the weather radar in Trappes from 1 Mar to 31 May 2008. (top) The differential reflectivity and (bottom) the number of analyzed sun signatures per day.

all differential reflectivity data in the scatterplot of Fig. 2. Note that the scatter pattern is remarkably circular, which suggests that the horizontal and vertical polarization lobes of the radar antenna are well matched. The sun-monitoring technique can thus be used to check the agreement between horizontal and vertical polarization lobes, which is a prerequisite for high-quality polarimetric measurements (Bringi and Chandrasekar 2001). The azimuthal and elevation curvatures for Trappes were determined as $a_x = a_y = 1.5 \pm 0.1 \text{ dB deg}^{-2}$. This implies that the vertical polarization lobes of the Trappes antenna are about 6% narrower than the horizontal polarization lobes. This difference is actually within the accuracy of the antenna beam pattern measurements that were performed with the installation of the radar. During the daily analyses, the curvatures have been fixed at this value to limit the number of fit parameters.

The available volume data from Trappes have been analyzed on a daily basis and the solar-monitoring results for a 3-month period are presented in Fig. 3. The results for the differential reflectivity are shown in the upper panel for both the sun-monitoring and rain calibration methods. The standard deviation of Z_{dr} during this period varies roughly between 0.2 and 0.4 dB for the solar monitoring and between 0.5 and 0.8 dB for the rain calibration. Typical standard deviations have been indicated for a single day by error bars in the figure. The daily differential reflectivity values from the solar monitoring are consistently positive, and some random fluctuations and step changes are seen during this 3-month period. The mean value over this period is 0.7 dB and the

standard deviation is 0.2 dB. Because the bandwidths for the horizontal and vertical polarizations are equal for the Trappes radar, this mean value is reflecting the receiver differential bias ΔR_{hv} .

For the rain calibration, only days with sufficient rain above the radar, about 50%, are shown in Fig. 3. The rain calibration of the differential reflectivity shows mostly negative values. The differential reflectivity bias derived from the rain calibration is -0.2 ± 0.3 dB. The good correlation between the sun-monitoring and rain calibration data is remarkable. The offset between the rain calibration and the sun-monitoring data is reflecting the transmitter differential bias. Thus, the good correlation implies that the transmitter differential bias is constant and the receiver differential bias is fluctuating. Currently, a correlation between this differential receiver bias and results of the electronic calibration every 2–3 days is being investigated. The mean offset is $\Delta T_{hv} = -0.6 \pm 0.2$ dB and this negative bias suggests that 13% less power is transmitted by the horizontal polarization channel.

The lower panel of Fig. 3 shows the number of sun signatures observed per day in the Trappes volume data. The most striking feature is the distinct 10-day oscillation observed during this 3-month period. Such an oscillation was not seen before for the Dutch and Finnish radars (Huuskonen and Holleman 2007; Holleman et al. 2010). A simple model was developed to simulate the number of sun signatures per day. Given the volume coverage pattern and the time offsets of all elevations with respect to the nominal scan time, all elevations and azimuths scanned per day by the radar antenna are simulated and the synchronized sun positions are calculated. The criterion for assigning a detected sun signature is based on the scatterplots of Fig. 2. The scatterplot is approximated by an ellipse centered at the calculated sun position with azimuth and elevation widths of 1.5° and 1.2° , respectively. When the simulated antenna orientation falls within this ellipse a sun signature is counted. The results of the simulations are also shown in the lower panel. The agreement with the observations is really good, and this evidences that the oscillation is due to characteristics of the employed volume coverage pattern and the local hemispherical trajectory of the sun.

b. Bornholm radar

The results from the daily sun monitoring of the Bornholm radar during April and May 2008 are presented in Fig. 4. The layout of the figure is similar to that of the previous figure. Before 20 May 2008, a slightly negative Z_{dr}^{sun} is seen with a mean value of -0.7 ± 0.2 dB. After a visit to the radar on 20 May for routine measurements, the differential reflectivity from the sun signatures dropped to -4.9 dB. The results of the differential

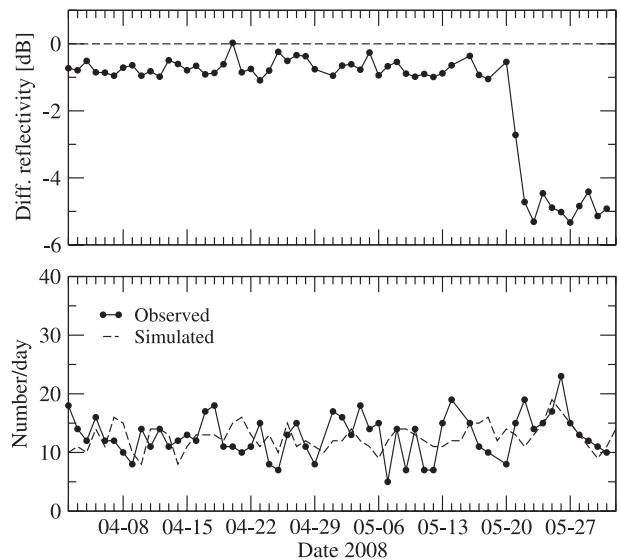


FIG. 4. As in Fig. 3, but for Bornholm from 1 Apr to 31 May 2008.

reflectivity monitoring were brought to the attention of the manufacturer (Enterprise Electronics Corporation; <http://www.eecradar.com/>). Follow-up investigations revealed that the calibration tables were inadvertently corrupted during the earlier visit by DMI staff. After a recalibration the problem was solved and the observed differential reflectivity of the sun returned to normal values.

The observed and simulated numbers of sun signatures per day are plotted in the lower panel of Fig. 4. No oscillation is seen for this radar because of the different volume coverage pattern, scan timings, and geographical location.

5. Summary and conclusions

The issue of differential reflectivity calibration is crucial for successful applications of polarimetric radar. Differential reflectivity measurements at vertical incidence can be used to calibrate Z_{dr} during rain events. Offline sun measurements, where operational scanning is stopped and the radar antenna is pointing at the sun, are generally employed to calibrate the polarimetric receiving chain. Here, we presented an online sun method for the monitoring of differential reflectivity from polarimetric weather radars. This online method allows for daily quality monitoring (independent of actual weather and using polar volume data) of operational polarimetric radars, which are becoming more and more abundant in observational networks.

The sun signatures contained in one month of volume data can be used to check the agreement between

horizontal and vertical polarization lobes of the radar antenna, which is a prerequisite for high-quality polarimetric measurements. For the polarimetric weather radar in Trappes it is found that these lobes are well matched and that the vertical polarization lobes of the antenna are about 6% narrower than the horizontal polarization lobes. By performing both the online sun monitoring and the rain calibration at vertical incidence, the differential receiver bias and differential transmitter bias can be disentangled. For the Trappes radar it is found that the differential transmitter bias is stable around -0.6 dB, whereas the differential receiver bias is fluctuating between 0 and 1 dB. An example from the polarimetric radar in Bornholm is shown to demonstrate the importance of regular monitoring of the differential reflectivity bias.

Because accurate calibration of the differential reflectivity is a prerequisite for most polarimetric algorithms, it is recommended that the online sun-monitoring method, which can be done independent of the actual weather, is performed daily on all polarimetric weather radars and networks thereof. Preferably this monitoring is performed in combination with the rain calibration at zenith.

Acknowledgments. Adriaan Dokter (KNMI) is acknowledged for assisting with the conversion of the Trappes volume data to the HDF5 format.

REFERENCES

- Bringi, V. N., and V. Chandrasekar, 2001: *Polarimetric Doppler Weather Radar*. Cambridge University Press, 636 pp.
- Gorgucci, E., G. Scarchilli, and V. Chandrasekar, 1999: A procedure to calibrate multiparameter weather radar using properties of the rain medium. *IEEE Trans. Geosci. Remote Sens.*, **37**, 269–276.
- Gourley, J. J., P. Tabary, and J. Parent du Châtelet, 2006: Data quality of the Meteo-France C-band polarimetric radar. *J. Atmos. Oceanic Technol.*, **23**, 1340–1356.
- Holleman, I., A. Huuskonen, M. Kurri, and H. Beekhuis, 2010: Operational monitoring of weather radar receiving chain using the sun. *J. Atmos. Oceanic Technol.*, **27**, 159–166.
- Huuskonen, A., and I. Holleman, 2007: Determining weather radar antenna pointing using signals detected from the sun at low antenna elevations. *J. Atmos. Oceanic Technol.*, **24**, 476–483.
- Melnikov, V. M., D. S. Zrnić, R. J. Doviak, and J. K. Carter, 2003: Calibration and performance analysis of NSSL's polarimetric WSR-88D. National Severe Storms Laboratory Tech. Rep., 72 pp. [Available online at http://publications.nssl.noaa.gov/wsr88d_reports/]
- Pratte, J. F., and D. G. Ferraro, 1989: Automated solar gain calibration. Preprints, *24th Conf. on Radar Meteorology*, Tallahassee, FL, Amer. Meteor. Soc., 619–622.
- Press, W. H., S. A. Teukolsky, W. T. Vetterling, and B. P. Flannery, 1992: *Numerical Recipes in C: The Art of Scientific Computing*. 2nd ed. Cambridge University Press, 994 pp.
- Ryzhkov, A. V., S. E. Giangrande, V. M. Melnikov, and T. J. Schuur, 2005: Calibration issues of dual-polarization radar measurements. *J. Atmos. Oceanic Technol.*, **22**, 1138–1155.
- Zrnić, D. S., V. M. Melnikov, and J. K. Carter, 2006: Calibrating differential reflectivity on the WSR-88D. *J. Atmos. Oceanic Technol.*, **23**, 944–951.